https://doi.org/10.5194/egusphere-2025-1830
Preprint. Discussion started: 21 May 2025

A Climate Intervention Dynamical Emulator (CIDER) for Scenario Space Exploration

Jared Farley[1], Douglas G. MacMartin[1], Daniele Visioni[2], Ben Kravitz[3,4], Ewa Bednarz[5,6], Alistair Duffey[7], and Matthew Henry[8]

[1]Sibley School of Mechanical and Aerospace Engineering, Cornell University, Ithaca, NY 14850, USA
[2]Department of Earth and Atmospheric Sciences, Cornell University, Ithaca, NY 14850, USA
[3]Department of Earth and Atmospheric Sciences, Indiana University Bloomington, Bloomington, IN 47405, USA
[4]Atmospheric Sciences and Global Change Division, Pacific Northwest National Laboratory, Richland, WA 99354, USA
[5]Cooperative Institute for Research in Environmental Sciences (CIRES), University of Colorado Boulder, Boulder, CO 80309, USA
[6]NOAA Chemical Sciences Laboratory, Boulder, CO 80309, USA
[7]Department of Earth Sciences, University College London, London, WC1E 6BS, United Kingdom
[8]Department of Mathematics, University of Exeter, Exeter, EX4 4PY, United Kingdom

Correspondence: Jared Farley (jf678@cornell.edu)

Abstract. Stratospheric Aerosol Injection (SAI) is a form of climate intervention that has been proposed as a way to reflect incoming solar radiation in order to provide a cooling effect and offset some of the impacts of greenhouse gas warming. Many possible scenarios for SAI implementation exist, ranging from steady, cooperative deployments across one or more injection latitudes to highly dynamic uncoordinated deployment with multiple independent actors with different aims. To explore the physical consequences across this wide range of possible SAI deployment scenarios, we develop the Climate Intervention Dynamical EmulatoR (CIDER), a climate emulator designed to emulate regional and global responses to a SAI deployment as the injection (or desired climate goals) vary in magnitude, latitude, and time. We train the emulator on existing sets of simulations from two Earth System Models. We then validate the emulator on a novel climate model simulated scenario of an example multi-actor uncoordinated SAI deployment. Our findings demonstrate that CIDER can be successfully used to estimate multiple climate variables of interest and across multiple climate models, including regional and global temperature and precipitation; it also successfully emulates results of an uncoordinated SAI deployment, rendering it an invaluable tool in exploring the climatic implication of a wide range of deployment scenarios, with the possibility of future coupling with regionally resolved integrated modeling frameworks in order to better quantify the potential societal impacts of SAI.

1 Introduction

Stratospheric aerosol injection (SAI) is a proposed method of solar radiation modification (SRM) that could cool surface temperatures (Budyko 1977, Crutzen 2006): the injection of aerosols or their precursors into the stratosphere, where they would scatter sunlight, increases the earth's albedo, and provides a cooling effect to the surface. SAI may be a tool to rapidly mitigate the effects of anthropogenic climate change due to rising greenhouse gas (GHG) concentrations. However, the specifics

https://doi.org/10.5194/egusphere-2025-1830
Preprint. Discussion started: 21 May 2025

of any particular SAI deployment (namely, location, timing, and magnitude of injections) will determine its overall impact on the climate. The flexibility in choosing when, where, and how to inject aerosols creates multiple degrees of freedom in SAI design. Those degrees of freedom might make SAI a versatile tool to manage more than just global mean temperature (Kravitz et al. 2016), but they also create a vast, difficult-to-analyze scenario space that complicates assessments of SAI (e.g. MacMartin et al., 2022).

The climate resulting from a given deployment depends on the details of SAI realization, including location, magnitude of injection, and how these change over time. These factors along with the background anthropogenic emissions together define the scenario space for SAI. For the most part, these factors (e.g. latitude, magnitude, and temporal evolution) have been explored separately. There is now a significant body of research using climate models to examine the effects of injection at different latitudes (Tilmes et al. 2017, Dai et al. 2018, Visioni et al. 2023, Bednarz et. al 2023, Zhang et al 2024, Henry et al. 2024), including estimating the number of meaningfully independent degrees of freedom (Zhang et al. 2022), designing strategies which fulfill multiple climate objectives at the same time (Kravitz et al. 2016, Kravitz et al. 2017, MacMartin 2017, Lee et al., 2020, Tilmes et al. 2018, Richter et al. 2022, Henry et al. 2023), and optimizing over different goals (Brody, Zhang et al. 2025). This research has largely looked only at the long-term response by averaging over several decades to examine its patterns. Scenarios have also explored the temporal dimension, including ramping up the injection rates over time to reach different temperature targets (Tilmes et al. 2020, MacMartin et al. 2022; Visioni et al, 2023b; Bednarz et al., 2023) or non-steady targets (MacMartin et al. 2014, Keith and MacMartin 2015, G6sulfur in Kravitz et al. 2015), changing the start date (Brody et al. 2024), and the effects of interruption, phase-out, or complete termination of deployment (Jones et al, 2013, Trisos et al. 2018, Farley et al. 2024). However, research on the temporal dimension of SAI deployment to this point has only considered a limited number of large-scale and long-term deployments.

The full scenario space for SAI includes cases with multiple latitudes of injection and the potential to change not only magnitude of injection rates but also injection latitude with time. A shift in latitudes could arise if a deployer's strategy changed, e.g., shifting from a high-latitude Arctic deployment (Lee et al. 2023) or dual-polar deployment (Bednarz et al., 2023a; Zhang et al., 2024) that can occur at relatively lower stratospheric altitudes to a more global one as high-altitude aircrafts became available (Wheeler et al 2025). Short term variations may be deliberately introduced as a response to a volcanic eruption (Laakso et al, 2016, Quaglia et al. 2024), or there may be other events that temporarily limit the ability to deploy at some latitudes but not others.

A significant class of scenarios that emerges from SAI's full scenario space is that of uncoordinated deployment. Multiple potential SAI deployers may exist simultaneously, and they may not agree on climate goals, may inject at the same or different latitudes, and may begin deployment at different times. Additionally, each actor can undergo its own difficulties in deployment and thus may interrupt or terminate independently (this aspect is particularly relevant with regards to external pressure put on an actor). Uncoordinated deployments of SRM are politically relevant and of substantial interest to the community of researchers studying SRM geopolitics (Weitzman 2015, Heyen et al. 2019, Meier and Traeger 2020, Sovacool et al. 2023, Keys and Bell 2023, Bell and Keys 2024, Diao et al. 2024, Morrissey 2024, McLaren 2025).

https://doi.org/10.5194/egusphere-2025-1830
Preprint. Discussion started: 21 May 2025

Comprehensively exploring the vast SAI scenario space with standard climate modeling tools (i.e., Earth System Models) is prohibitively computationally expensive. However, a potential solution to this barrier is to use climate emulators. An emulator is a model of reduced complexity that captures the primary desired features of climate model output at a tiny fraction of the computational cost. Climate emulators have been used for the purpose of exploring climate change scenarios (Tebaldi et al. 2022), and multiple emulators for warming-related projections have been developed (Smith et al. 2018, Nath et. al. 2022).

Recently, climate emulators have also been discussed as a tool to explore the SRM scenario space and its climate responses (MacMartin and Kravitz 2016). In Farley et al. (2024), we developed a climate emulator for SAI capable of connecting rates of injections of SO_2 with global mean temperature and precipitation response to explore a wider variety of scenarios. Here we describe the development and validation of the Climate Intervention Dynamical EmulatoR (CIDER), which is designed to emulate the regional effects of SAI as it varies in latitude, magnitude, and time. In doing so, we have created a tool that can rapidly explore the diverse scenario space of SAI for large-scale climatic variables relevant to understanding tradeoffs associated with scientific and geopolitical questions about potential SAI deployments. Additionally, we validate this emulator on a novel climate model simulation of an example multi-actor uncoordinated SAI scenario. Section 2 provides an overview of CIDER's formulation and dynamical equations (Section 2.1), details the parameter-training methodology for the emulator and describes the data used for training on two different climate models (Section 2.2), and describes the novel uncoordinated scenario (Section 2.3). Section 3 assesses how well CIDER captures the climate responses simulated by Earth System Models (ESMs), both to coordinated and uncoordinated SAI. Finally, Section 4 discusses its use cases and limitations.

2 Brewing CIDER (Methods)

2.1 Emulator Overview

The purpose of CIDER is to calculate a time series of 2-dimensional (latitude and longitude) patterns of climate variables, given a set of user-specified inputs for the time-series of SO_2 injection rates across multiple latitudes; the emulator is trained using simulation data from one or both climate models, with individual parameters for each. The emulator currently calculates monthly mean near-surface air temperature (T), precipitation (P), and evaporation (E) patterns, but the methodology can be expanded for other variables provided that their response to SAI forcing can be reasonably approximated as linear. CIDER completes these calculations in four steps, which we briefly summarize here and then expand upon later:

1. First, the emulator calculates the value of global mean stratospheric Aerosol Optical Depth (AOD) in response to the user-provided injection of specified amounts of SO_2 at different latitudes.

2. The emulator computes global mean climate variables changes in response to anthropogenic changes in radiative forcing using both CO_2 equivalent data for the Shared Socioeconomic Pathway (SSP) scenarios from Meinshausen et al. (2020) as underlying global warming scenarios, and stratospheric AOD derived from step 1.

https://doi.org/10.5194/egusphere-2025-1830
Preprint. Discussion started: 21 May 2025

3. The emulator then calculates spatial patterns of climate variables responses derived from single injection location cases for SAI and combines them in a linear way to match the simulated AOD given as input from the SO_2 injections, as well as adds the predetermined GHG forcing changes.

4. Finally, the emulator scales the spatial patterns obtained by the magnitude of global stratospheric AOD and GHG forcing changes, assuming linearity in these responses, and adds the patterns together.

A diagram of this process is shown in Fig. 1.

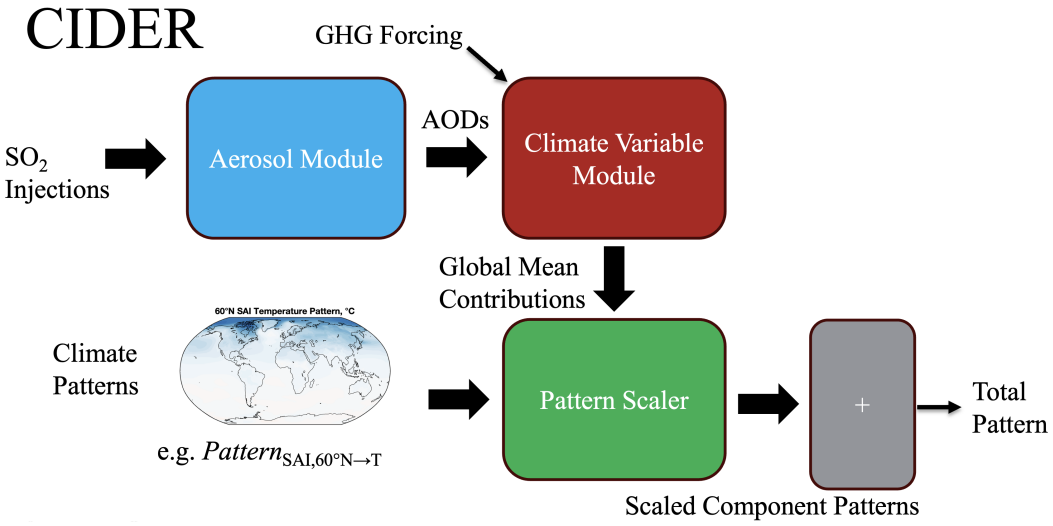

Figure 1. Diagram showing CIDER's modules. For each latitude, injection time series are input into the aerosol module, and the module generates global mean AOD time series. These are then input, along with a timeseries of GHG forcing, to model the dynamics of each climate variable (e.g. temperature or precipitation) included in CIDER. Their contributions to the global mean are calculated, and the climate variable pattern from each injection latitude is scaled by the respective contribution. These scaled patterns are then added together to provide the total global pattern in response to the aerosol injection and change in GHG concentration.

The available injection latitudes in CIDER are 60°N, 30°N, 15°N, 0°N, 15°S, 30°S, and 60°S. The reasoning for restricting the injection latitudes space to these locations is explained in depth in Zhang et al. (2023): briefly this is a sufficient set in CESM2(WACCM) to capture the range of possible responses to SAI with injections at any location in the sense that any other injection choice can be adequately expressed as some combination of these.

The dynamic responses of AOD to injection (Step 1) are calculated by convolving the impulse responses of AOD to injection. The impulse response of the global mean AOD to injection at any particular latitude takes the form

$$g(t) = \beta e^{-(\alpha+\gamma\cdot q(t))\cdot t} \quad (1)$$

where β is a scaling capturing the equilibrium response to injection, α is the time constant, and γ is a parameter to capture the nonlinear response based on the magnitude of injection rate q(t). β and α are components of the linear response, and the

https://doi.org/10.5194/egusphere-2025-1830
Preprint. Discussion started: 21 May 2025

sublinear response of AOD to injection rate is the most important nonlinearity to capture (via γ). All three of these parameters depend on the injection latitude. The response of AOD at some time t (in months) depends on injections at that latitude up to time t, and is thus

$$AOD(t) = \sum_{j=1}^{t} g(j) \cdot q(t-j) \tag{2}$$

The global mean climate responses to changes in GHGs and AOD (Step 2) are calculated similarly, by convolving the impulse responses of the climate variable of interest to AOD or GHG forcing. The global mean response is modeled as semi-infinite diffusion, which has been used previously in climate emulators (Hansen et al. 1984, Caldeira and Myhrvold 2013, MacMartin et al. 2014, MacMartin and Kravitz 2016, Farley et al. 2024). Its impulse response is of the form

$$h_{x\to y}(t) = \mu_{x\to y}\left(\frac{1}{\sqrt{\pi t \tau^*_{x\to y}}} - e^{\frac{t}{\tau^*_{x\to y}}} erfc\left(\sqrt{\frac{t}{\tau^*_{x\to y}}}\right)\right) \tag{3}$$

where x is a particular forcing input, y is the climate variable of interest, t is months since the emulation's start, $\tau^*_{x\to y}$ determines the time scale of the response, and $\mu_{x\to y}$ is a scaling factor capturing the equilibrium climate response to the forcing input. $\mu_{ghg\to T}$ has units °C·(Wm^{-2})$^{-1}$ and $\mu_{ghg\to P}$ has units mm/day·(Wm^{-2})$^{-1}$. Likewise, $\mu_{sai\to T}$ has units °C·(unit AOD)$^{-1}$ and $\mu_{sai\to P}$ has units mm/day·(unit AOD)$^{-1}$, for all latitudes of SAI deployment. The response at time t of any climate variable to a given forcing is thus,

$$y_x(t) = \sum_{j=1}^{t} h_{x\to y}(j) \cdot f_x(t-j) \tag{4}$$

where $f_{sai,lat}$ is the AOD above baseline for a particular latitude and f_{ghg} is described as in Myhre et al. 1998:

$$f_{ghg}(t) = 5.35 ln\left(\frac{CO_2(t)}{CO_2(reference)}\right) \text{W m}^{-2} \tag{5}$$

At this stage, the overall global mean response can be obtained by summing the contributions y_x from each individual forcing. However, to get the projection of that global mean into a global pattern, two more steps are needed.

Step 3 proceeds with simple pattern scaling on all the individual responses:

$$Y_x(t) = y_x(t) \cdot Pattern_{x\to y} \tag{6}$$

where the two-dimensional climate variable pattern for a forcing x (denoted $Y_x(t)$) is defined as the product of the time-varying global mean $y_x(t)$ (as above) and a time-invariant spatial pattern of that variable $Pattern_{x\to y}$ that depends on the forcing (GHGs or a specific latitude of SO_2 injection). Pattern scaling has a long history of use in climate model emulation and, for a wide variety of situations, is accurate in reproducing large-scale Earth System Model output (e.g. Santer, 1990; Kravitz et al., 2017).

Step 4 adds the 8 scaled patterns (7 latitudes of injection + GHG warming) together to produce the net change in the climate variable of interest. This relies on two different linearity assumptions, widely tested but here combined for the first time; a

https://doi.org/10.5194/egusphere-2025-1830
Preprint. Discussion started: 21 May 2025

pattern scaling one for GHG normally used in climate emulators (from Santer et al., 1990 to Tebaldi et al., 2022), and an assumption that different patterns of cooling from SAI can be combined linearly, tested for SAI from MacMartin et al. (2017), up to Brody et al. (2025). The resultant pattern is CIDER's estimation of the pattern of that climate variable at that time due to the forced responses of SAI and GHG.

2.2 Emulator Training

For each latitude x of SAI deployment available in CIDER, the following parameters must be trained: α_x, β_x, γ_x, which model the relationship between injection rate and global mean AOD; $\mu_{x\to y}$, $\tau_{x\to y}$, which model the global mean response of a particular climate variable y to the AOD resulting from injection at latitude x; and Pattern$_{x\to y}$, which projects the pattern of the global mean response of that variable onto the globe.

To train the three parameters that describe the global mean AOD response to injection at a particular latitude, we use two simulation types (at least one ensemble member per type). The first is the response to a step increase in injection rate at a single latitude (from 0 Tg SO_2/year to a fixed 12 Tg SO_2/year), whose clear signal gives sufficient information to estimate α_x and β_x, the time constant and the equilibrium response. However, it gives no information about γ_x, the nonlinear dependence on injection magnitude, since it injects only at a single rate. The second simulation type we run is to train γ_x. We need a simulation with a range of injection rates at a particular latitude; for this we use strategies that maintain a constant temperature target with increasing climate change through symmetric injection about the equator. Since these simulations increase the cooling done over time, they provide a good range of injection rates for training. While training on these hemispherically-symmetric injections, we assume that the AOD resulting from simultaneously injecting at latitudes in opposite hemispheres can be added linearly; this linearity was shown in MacMartin et al. (2017). With these two sets of simulations' corresponding injection logs as input, we can find the parameters α_x, β_x, and γ_x by minimizing the root mean square error between CIDER's AOD estimation and the simulated AOD. For a full list of simulations, see Table 1.

The parameters $\mu_{x\to y}$ and $\tau_{x\to y}$ are found in a similar manner. We optimize a least-squares fit for each latitude of SAI in CIDER, using the simulations with a step injection of 12 Tg SO_2/year. We use these simulations' global mean AOD as input and global mean values of the climate variable (emulation vs. simulation) as output. To find Pattern$_{x\to y}$, the climate pattern associated with each latitude, we average the pattern of the climate variable over the last 20 years of that latitude's step response. For finding the climate response to greenhouse gas forcing, the parameters from injection to AOD are ignored and the forcing is used as in Fig. 1 – the background emissions scenario for all training simulations used is SSP2-4.5, the moderate Shared Socioeconomic Pathway that is roughly consistent with the Nationally Determined Contributions of the Paris Agreement (Burgess, 2021). When climate variability is needed (e.g., for Figs. 3 or 6), a long pre-industrial simulation is used to calculate and generate it (Davis et al., 2023); this assumes that the statistics of variability do not change. For a full list of simulations used, see Table 1.

Two climate models are used to train and test CIDER's parameters and performance. One is the fully-coupled Community Earth System Model version 2 with the Whole Atmosphere Community Climate Model version 6 (CESM2-WACCM6) (Danabasoglu et al., 2020) with middle atmosphere chemistry (Davis et al., 2023) and a high top (~ 140 km). Its meridional res-

https://doi.org/10.5194/egusphere-2025-1830
Preprint. Discussion started: 21 May 2025

olution is 0.95°, its zonal resolution is 1.25°, and it uses 79 vertical layers extending up to 10^{-5} hPa. For CESM2-WACCM6, pre-industrial (PI) temperature is defined as in MacMartin et al. (2022), with 2020-2039 average global mean temperature defining 1.5°C above PI. The other model used is UKESM1.0 (Sellar et al. 2019), using HadGEM-GC3.1 (Kuhlbrodt et al. 2018) as its atmosphere-land-ocean-sea ice model with the Met Office Unified Model (UM) as its atmospheric component, United Kingdom Chemistry and Aerosol (UKCA) chemistry model (Mulcahy et al. 2018; Archibald et al., 2020) as its chemistry model with troposphere-stratosphere chemistry and coupling to a multi-species GLOMAP modal aerosol scheme (Mann et al. 2010). Its meridional resolution is 1.25°, its zonal resolution is 1.875°, and it has 85 vertical layers extending up to 85 km. Pre-industrial is defined as in Henry et al. (2023), with 2014-2033 average global mean temperature defining 1.5°C above PI.

2.3 Simulation of Uncoordinated SAI

We run an example of a highly dynamic scenario of uncoordinated SAI deployment in CESM2, both to provide validation data for this emulator (and others in the future) and to analyze on its own merits. To do this, we run a three-member ensemble using the fully-coupled CESM2-WACCM6, with the settings specified as in Davis et al. 2023.

In this scenario, we have three actors deploying SAI, as detailed in Table 2; this includes (i) an actor injecting at 60°N to cool the Arctic, (ii) a second actor injecting at the equator to reduce global mean temperature, and (iii) a third actor in the southern hemisphere aiming to avoid disrupting tropical precipitation. This scenario is but one representative of the infinite design space of uncoordinated scenarios. In selecting this scenario, we make no claims regarding geopolitical plausibility or the likelihood of it occurring; rather, this scenario captures a number of relevant features unique to the space that may lead to interesting climate dynamics:

1. All three actors have different climate targets - regarding both the region of interest and targeted value (defined here as the average value over a 20-year period centered on a reference year).
2. The Arctic actor begins deployment before the others, since polar SAI may be easier logistically (Smith et al. 2022, Wheeler et al. 2025).
3. The actor wanting a balanced N-S Temperature gradient (for purposes of controlling the behavior of the Inter-Tropical Convergence Zone, see Kravitz et al. 2016) deploys in the hemisphere opposite to the Arctic actor but is delayed in their start.
4. The actor targeting global mean temperature terminates permanently mid-deployment (the reason is not relevant to the scenario specification). The ability for other actors to respond is limited but non-zero.
5. The remaining actors transition out of non-coordination to a coordinated, hemispherically-symmetric deployment, following the termination of Actor 2. However, this process takes time.

Since this scenario was developed in part to provide validation data for CIDER, injection totals were determined by using CIDER, and no feedback controller was used in the simulation, even if the targeted value would otherwise stray (e.g. if

https://doi.org/10.5194/egusphere-2025-1830
Preprint. Discussion started: 21 May 2025

Table 1. List of simulations used in this paper for both training and validating the emulator.

Title	Latitude	Injection Strategy, Starting 2035	Ens. Size	Used to . . .	Source
Pre-Industrial	N/A	N/A	1	Calculate Variability	Davis et al. 2023
SSP2-4.5	N/A	N/A	3	Train Climate Response	MacMartin et al. 2022
Single-Point-30N Single-Point-15N Single-Point-0N Single-Point-15S Single-Point-30S	30°N 15°N 0°N 15°S 30°S	12 Tg total, constant	3	Train AOD and Climate Response	Zhang et al. 2022, Visioni et al 2023a, Bednarz et al. 2022
Single-Point-60N Single-Point-60S	60°N 60°S	12 Tg, boreal spring 12 Tg, austral spring	1	Train AOD and Climate Response	Zhang et al. 2022, Lee et al 2023
Target-1.0-0N Target-1.0-15NS Target-1.0-30NS	0°N 15°N + 15°S 30°N + 30°S	Global mean temperature to 1.0°C above PI for CESM2, 1.5°C above PI for UKESM1	3	Train AOD	Zhang et al. 2024, Bednarz et al. 2023a, Henry et al. 2024
Target-1.0-60NS	60°N + 60°S	Global mean temperature to 1.0°C above PI, injected in hemisphere's spring at 15 km for CESM2, 1.5°C above PI injected year-round at 22 km for UKESM1	3	Train AOD	Zhang et al. 2024, Bednarz et al. 2023a, Henry et al. 2024
Multi-Obj-1.5 (CESM) Multi-Obj-1.0 Multi-Obj-0.5	30°N + 15°N + 15°S + 30°S	T0+T1+T2 to 2020-2039 levels T0+T1+T2 to 2008–2027 levels T0+T1+T2 to 1993–2012 levels	3	Validate	MacMartin et al. 2022
Multi-Obj-1.5 (UKESM1)	30°N + 15°N + 15°S + 30°S	T0+T1+T2 to 2014-2033 levels	3	Validate	Henry et al. 2023
Uncoordinated	60°N + 30°N + 0°N + 30°S	See Section 2.3	3	Validate	This paper

https://doi.org/10.5194/egusphere-2025-1830
Preprint. Discussion started: 21 May 2025

overcooling occurred in the Arctic), and the injection inputs to CESM2 and CIDER are identical. Additionally, the following simplifications and assumptions are applied during the uncoordinated period:

- Actors deploy using integer amounts of Tg/year.
- Actors can increase their injection capacity by at most 1 Tg/year per year.
- As the scenario progresses, Actor 1 phases out injection as it is no longer needed to maintain its target, however it keeps half of its maximum 60°N injection capacity at the ready (8 Tg halved to 4 Tg). It can deploy it after a 1-year lag.
- It takes roughly 5 years to develop the capacity to deploy SAI in non-polar regions.

Table 2. Uncoordinated SAI actors and goals.

Actor #	Deployment Latitude	Initiation year	Uncoordinated Goal	Additional Notes
Actor 1	60°N	2035	Arctic mean temperature to 2020 level	
Actor 2	0°N	2040	Global mean temperature to 2000 level	Terminates in 2053 (after ramping up to 13 Tg SO_2/yr)
Actor 3	30°S	2042	N-S Temperature Gradient to 2035 level	
Actor #	Deployment Latitude	Initiation year	Coordinated Goal	Additional Notes
Actor 1+3	30°N + 30°S	2058	Global mean temperature to 2020 levels	Builds towards symmetric injection rates (beginning in 2065)

We choose for Actor 2 to undergo a termination in 2053. In response, Actor 1 redeploys half its capacity after its 1-year lag. Then, we choose for Actors 1 and 3 to begin coordinating and agree to deploy a coordinated symmetric deployment. Actor 1 begins developing capacity to inject at 30°N, to match Actor 3's 30°S; it begins developing capacity in 2053, begins deployment in 2058, and reaches symmetry with Actor 3 in 2065.

Validations using this uncoordinated scenario are presented in Fig. 5 and discussed in Section 3.

3 Sampling CIDER (Results)

CIDER currently is able to estimate AOD, temperature, precipitation, and evaporation (evaporation in Appendix A1). The results of the training and testing of CIDER using CESM2-WACCM6 results are shown in Fig. 2. Figures 2g, 2h, and 2i show the emulator's validation against SAI scenarios which use injection across four latitudes to fulfill three objectives simultaneously (global mean temperature, N-S temperature gradient, and equator-to-pole temperature gradient – see MacMartin et al.

https://doi.org/10.5194/egusphere-2025-1830
Preprint. Discussion started: 21 May 2025

2022). The emulator fits the global mean AOD, temperature, and precipitation of these multi-objective scenario simulations for 1.0°C above PI with a root mean square error (RMSE) of 0.01 AOD, 0.075°C, and 0.01 mm/day, respectively. For reference, the year-to-year standard deviation of temperature is 0.12°C and of precipitation is 0.015 mm/day. AOD variability is harder to calculate, since much of its variability is driven by the year-to-year injection of the feedback controller, but CIDER overestimates AOD by about 5%.

We see undercooling in the scenario for 1.5°C above PI and overcooling in the scenario for 0.5°C above PI (13% undercooling and 8% overcooling). As the runs it trained on for temperature injected 12 Tg-SO_2 for roughly a degree of cooling, CIDER fits the multi-objective run with most similar injection and cooling the best; any nonlinearities in the system cause error to grow as the amount of injection and the scenario's target stray from the values included in the training. Similar behavior appears in precipitation, with under-reduction of precipitation 1.5°C above PI and over-reduction of precipitation 0.5°C above PI. The limitations of the linear approximation in capturing CESM2's nonlinearity in cooling also appeared in Farley et al. 2024, though the emulator in that paper had no pattern scaling.

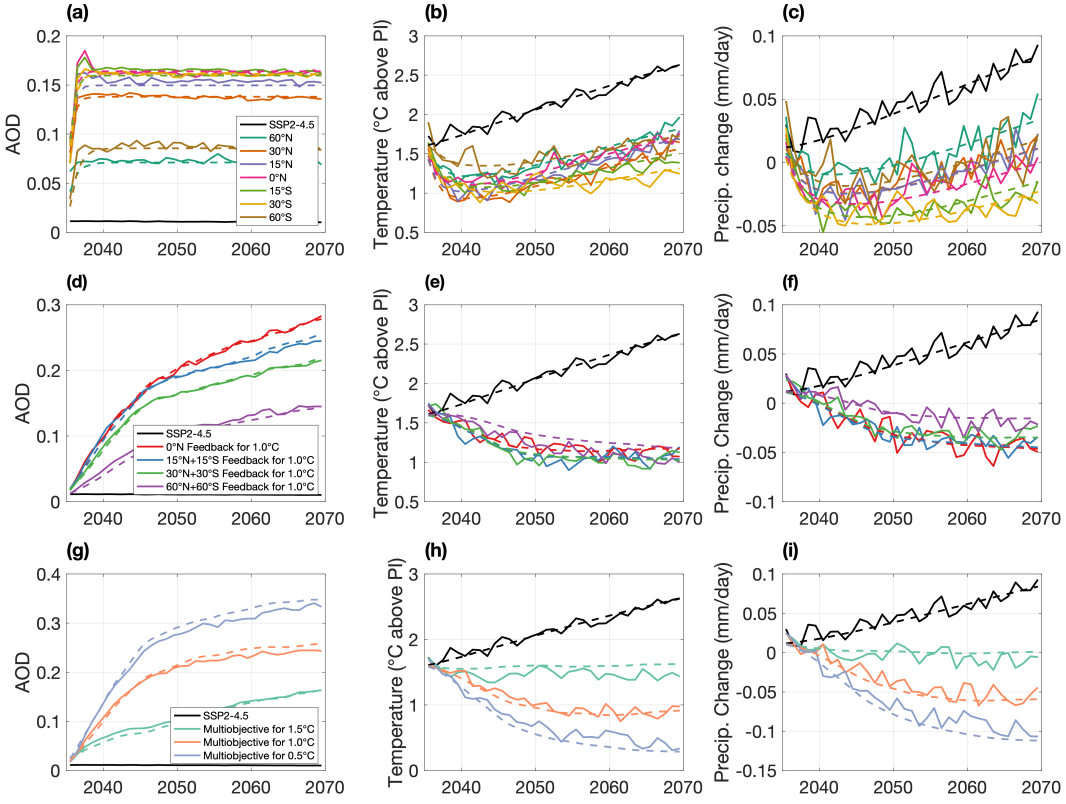

Figure 2. CESM2 (solid line) global mean responses of AOD (a,d,g), near-surface air temperature above pre-industrial (b,e,h), and precipitation change from 2020-2039 average (c,f,i), along with CIDER emulations of the same (dashed line). Plots a, b, and c show the responses of the fixed injection (training data), plots d, e, and f show the responses of the symmetric injection runs for 1.0°C above PI (also training data), and plots g, h, and i show the responses of the multi-objective runs (validation data).

https://doi.org/10.5194/egusphere-2025-1830
Preprint. Discussion started: 21 May 2025

Figure 3 examines the difference between the CIDER and CESM2 temperature and precipitation patterns for a multi-objective scenario. It also compares this with simply scaling a multi-objective scenario of a different temperature target (a simpler but less flexible approach). In 3a and 3b, the multi-objective for 1.0°C above PI scenario CIDER emulation was subtracted from the CESM2 simulation of the same scenario (a 3-member ensemble), and then in 3c and 3d the mean of those differences was normalized by the standard error at each grid cell. In 3e and 3f, the cooling pattern of multi-objective for 1.5°C above PI scenario was scaled to 1.0°C above PI, and then the subtraction and normalization by standard error was conducted as in 3c and 3d. In both temperature and precipitation, CIDER provides comparable performance to the estimation of the 1.0°C above PI scenario as the scaling of 1.5°C above PI.

A notable difference, however, is the large cooling spot in the Northern Atlantic Ocean. CIDER does not model Atlantic Meridional Overturning Circulation (AMOC) dynamics, and the patterns which it is scaling are those of the 12 Tg SO_2 step responses. The difference in the Northern Atlantic is likely due to the more rapid cooling of the step responses that leads to a more rapid effect on the slowing of AMOC in a way that the gradual ramp-in cooling from the multi-objective case does not (Bednarz et al., 2025, in review). This interaction with AMOC dynamics is captured in the patterns used in CIDER, so it creates an error in this region when emulating strategies that gradually ramp-in cooling. Future versions of CIDER could include the AMOC dynamics pattern separately to correct this limitation.

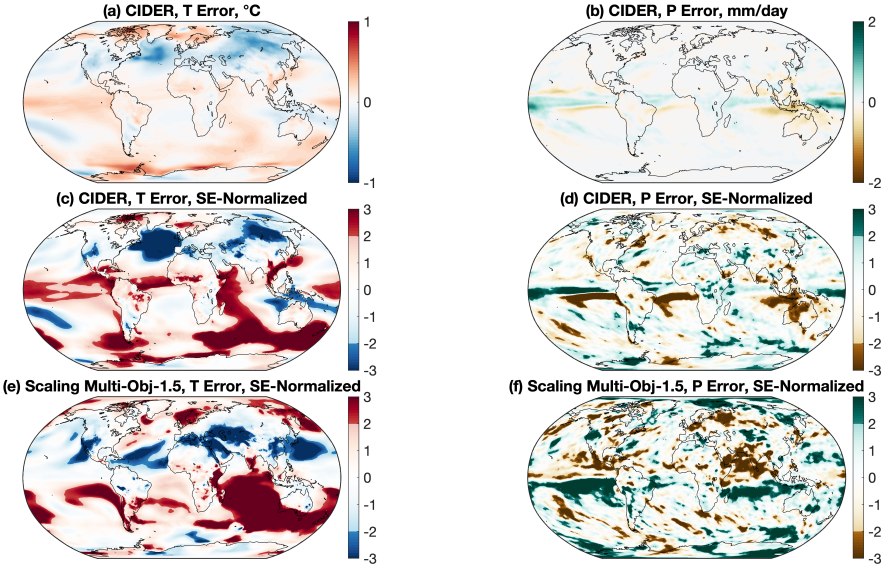

Figure 3. Error in pattern matching the multi-objective for 1.0°C above PI scenario. A difference was taken over the last 20 years of the scenario (CESM2 3-member ensemble - CIDER emulation) for temperature (a,c) and precipitation (b,d). For plots c and d, the plots for a and b were normalized by the standard error of the grid cell's values, calculated over the last 20 years of the scenario. Grid cells less than two standard errors from the norm are whitened. For plots e and f, the pattern of cooling for the multi-objective for 1.5°C above PI scenario was scaled by CIDER's global mean cooling and then subtracted in a similar manner to c and d to provide a comparison.

https://doi.org/10.5194/egusphere-2025-1830
Preprint. Discussion started: 21 May 2025

Figure 4 replicates Fig. 2, but it uses UKESM1 in place of CESM2. CIDER's aerosol module does slightly worse with the nonlinearity present in UKESM1's aerosol dynamics (as discussed already in Visioni et al. (2023)) - at higher injection rates, the AOD increases more slowly with increased injection rate. Additionally, the uncaptured nonlinearity to cooling in temperature and precipitation (especially the dual-polar 60°N and 60°S deployment) is more prevalent near the ends of runs in 4e and 4f, where there is larger injection to offset the GHG forcing. It is likely that the good emulation of the multi-objective runs' temperature (4h) and precipitation (4i) is the overestimation of AOD compensating for the underestimation of the climate variable's response to forcing. While the resultant emulation achieves a correct result, it should be treated with a degree of caution (especially if one wants to extrapolate into the future, as those errors may not cancel anymore). Use of an aerosol module with zonal resolution, such as the one in Aubrey et al. 2020 or Toohey et al. 2025, may aid performance in capturing the nonlinear aerosol behavior.

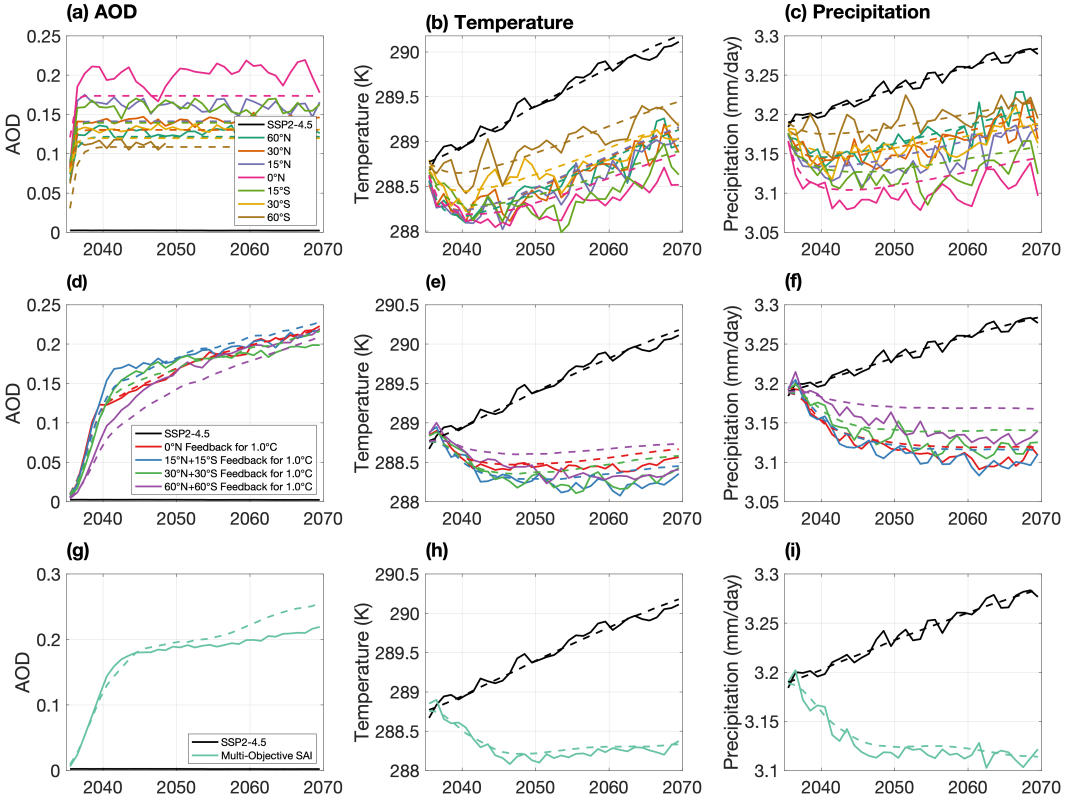

Figure 4. UKESM1 (solid line) global mean responses of AOD (a,d,g), temperature (b,e,h), and precipitation (c,f,i), and CIDER emulations of the same (dashed line). Plots a, b, and c show the responses of the fixed injection, plots d, e, and f show the responses of the symmetric injection runs for 1.0°C above PI, and plots g, h, and i show the responses of the multi-objective run.

Figure 5 displays the results of the multi-actor uncoordinated scenario described in Section 2.3. We compare CIDER's emulation of the scenario to the simulation in CESM2, using the injection rates in Fig. 5a as input to both. Overall, when

https://doi.org/10.5194/egusphere-2025-1830
Preprint. Discussion started: 21 May 2025

comparing global mean AOD (5b), global mean (5c) and regional (5d) temperature, and global mean precipitation (5f), CIDER matches the output of CESM2. For Fig. 5e, although the behavior of both CIDER and CESM2 is similar, CIDER as currently trained seems to have an offset bias towards a warm north and cool south – this can also be seen in Fig. 3c and is likely due to the ocean dynamics that CIDER does not capture. As for the simulation itself, it is evident how each actor's behavior affects not only their progress to their own target but also others' progress towards theirs. Even though Actor 1 and 2 are not coordinating, Actor 1 is pressured to phase out their deployment as Actor 2 phases in in order to avoid overcooling (and possibly should have phased out slightly quicker). Likewise, Actor 3's progress to their N-S temperature gradient goal is in part because they deploy in the southern hemisphere, but it is also in part because Actor 1 phases out their northern hemisphere deployment (a phase-out Actor 1 performs in response to Actor 2). The deployments of the three actors are intertwined. ~~As a note,~~ while in this scenario Actors 1 and 3 each put aside their individual uncoordinated goals when transitioning to the coordinated symmetric 30°N+30°S deployment for 1.0°C above PI, there is a non-symmetric strategy that fulfills all 3 goals (see Appendix A2).

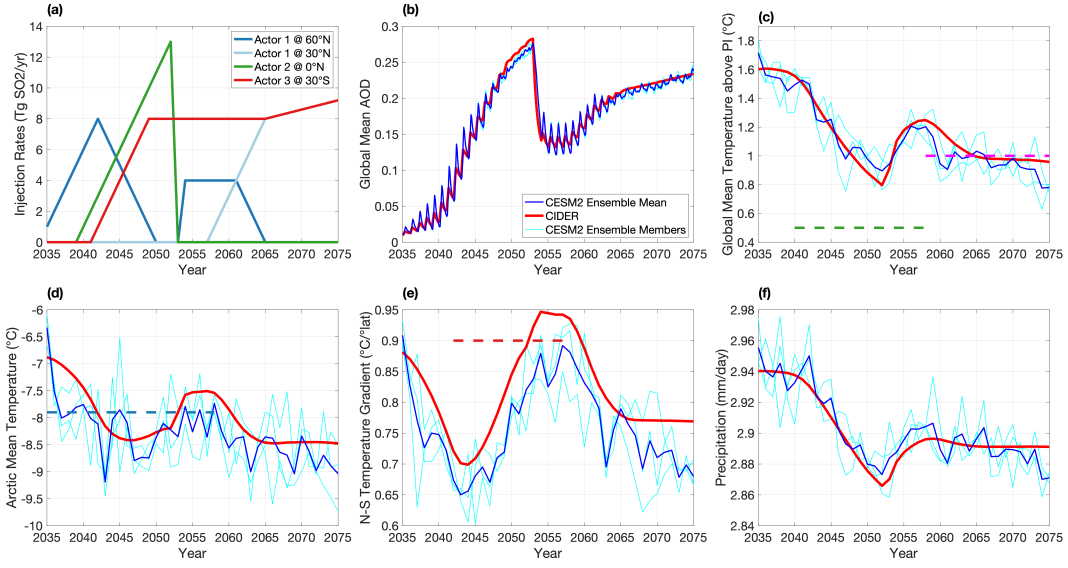

Figure 5. Example multi-actor uncoordinated scenario in CESM2 and emulated with CIDER. (a) The annual injection rates to accomplish the goals set in Table 2. (b) Global mean AOD. A sharp drop occurs following Actor 2's termination in 2053. (c) Global mean temperature. Dashed green line indicates Actor 2's goal (which is not met prior to their termination), and dashed magenta line indicates Actor 1+3's coordinated goal for 2055-2075. Note the sharp but limited increase in temperatures resulting from Actor 2's termination. (d) Arctic mean temperature. The dashed blue line indicates Actor 1's goal. Note the minor overcooling that occurs because Actor 1 does not phase out quick enough during Actor 2's phase-in. (e) N-S temperature gradient (as defined in Kravitz et al 2016). The dashed red line represents Actor 3's goal. The gradient quickly lowers as Actor 1 deploys in the Arctic, and it rises again as both Actor 3 deploys at 30°S and Actor 1 phases out to maintain 2020 Arctic temperature (rather than over-cooling). (f) Global mean precipitation. Global mean precipitation was no one's target during this simulation.

https://doi.org/10.5194/egusphere-2025-1830
Preprint. Discussion started: 21 May 2025

Additionally, we can combine CIDER's estimate of the forced response to SAI with simulations of climate internal variability. This combination gives emulations of SAI that include spatially and temporally coherent patterns of variability, which can be useful for analysis. Results of this combination, as well as the CESM2 simulations it is emulating, are shown in Fig. 6.

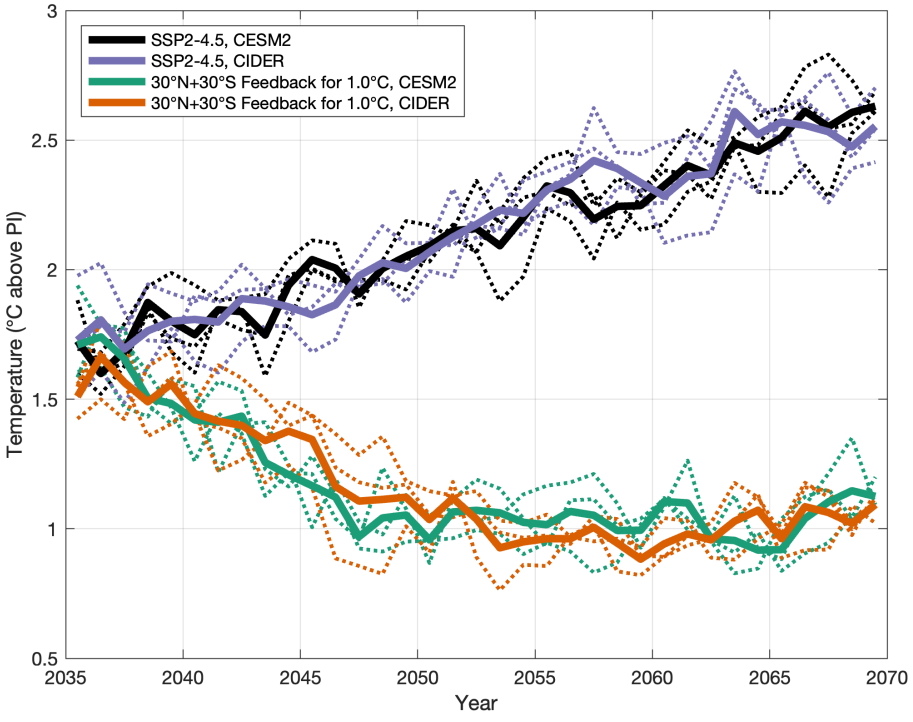

Figure 6. Adding interannual variability to the emulation. Variability is taken from a random subset of simulation of pre-industrial conditions, removing the mean, and then added onto CIDER's emulation. The solid line is CESM2 simulation; the dashed line is the CIDER emulation.

4 Mulling CIDER (Conclusions)

In this paper, we described our design and validation of the Climate Intervention Dynamical EmulatoR ~~(CIDER)~~, a climate emulator capable of simulating a wide array of potential future scenarios including Stratospheric Aerosol Injection ~~(SAI).~~ Through the input of GHG concentrations and SAI injection of sulfate precursors at different latitudes, CIDER outputs spatially and temporally resolved maps (response as a function of latitude, longitude, and time) of forced responses in surface climate variables (currently those of temperature, precipitation and evaporation) to climate change and SAI. CIDER can be trained to emulate multiple climate models provided the right set of simulations is used for training (e.g., Visioni et al., 2023; Bednarz et al., 2022). In addition, we used results from CESM2 and UKESM1 to demonstrate the flexibility of the framework. CIDER

https://doi.org/10.5194/egusphere-2025-1830
Preprint. Discussion started: 21 May 2025

output can be used in analysis of a diverse set of SAI scenarios, including quickly-varying and uncoordinated deployment from multiple actors. Since CIDER is computationally inexpensive enough to be run on a laptop or website (on the order of a few seconds or less), we expect this model to be useful for various purposes, such as in real-time climate games and workshops (e.g., Rooney-Varga et al. 2020, Pereira et al., 2021), and in scenario exploration and generation, potentially in conjunction with economic models (Andreoni et al., submitted). This process can identify a subset of scenarios where it may be valuable to conduct fully-coupled climate model simulations to better evaluate outcomes. CIDER can provide dynamically-grounded feedback on how generated scenarios would behave, and that feedback would allow participants or simulated actors to evolve their strategies in turn. This social-physical cycle may more closely resemble how climate decisions will be made in the real world, where climate models, decision-making, and impacts are interconnected.

Here, we validated CIDER against both "well-behaved" scenarios—scenarios which are conceived to be the work of a single actor controlling for a few (three) objectives (though these same scenarios could easily also be thought of as three actors independently controlling for one objective each, due to the structure of the control algorithm)—and against a scenario which is designed to be "poorly behaved", including conflicting goals, staggered start times for different actors, and terminations of one but not all actors. For clarity, CIDER captures neither who deployed a particular injection of SO_2 nor why they did so—the longitude of an injection is not a part of CIDER's input, and the emulator estimates only the physical climate variables and AOD with respect to a particular set of injection rates. That said, CIDER is designed with the intent of interfacing with methods of choosing SAI injection and GHG concentration pathways that incorporate feedback to climate outcomes.

The most potentially valuable use of CIDER is in those non-standard scenarios that are very different from what has typically been simulated in SAI research to date. As we see in Fig. 3, one can achieve similar performance in estimating the multi-objective 1.0°C above PI scenario by scaling the cooling of the 1.5°C above PI scenario as an analog. However, a pure scaling-based approach can only be used to project outcomes from increasing or decreasing a target relative to an existing simulation, and can't capture the behaviour of any scenario involving either a different spatial distribution of injection rates, a different temporal evolution, or both. The changes of the N-S temperature gradient (as seen in Fig. 5e) as actors in the north and south phase-in and phase-out deployment is a potentially very significant feature of interest, considering that the N-S temperature gradient influences the behavior of the Intertropical Convergence Zone. Additionally, one actor's deployment of SAI (and the choices they make) can influence the deployment of all the other actors, even if they aren't cooperating, in highly divergent ways, since everyone is injecting into the same world. Hence, the deployment decisions still interact through the climate response. If we wanted to simulate a similar scenario but with different goals or injection locations or events, it would in general result in a very different outcome (in both injection input and climate output). Since CIDER is computationally inexpensive, it can be used in explorations of a scenario space that examine many novel and highly varying scenarios. To run this large set of scenarios with varied parameters in a climate model would likely be prohibitively computationally expensive. To run such a set of scenarios in CIDER is basically free.

By design, CIDER dynamically emulates only the forced response to GHG and SAI. In being able to estimate regionally-resolved forced precipitation and temperature (as well as any other climate variable that scales as they do), it can be used for a variety of assessments of risks. Nevertheless, it could be useful to add in additional variability to account for additional

https://doi.org/10.5194/egusphere-2025-1830
Preprint. Discussion started: 21 May 2025

potential responses to behaviors, for example, a nation perceiving failure and thus changing their injection behavior (Keys et al., 2022). Figure 6 shows the dynamical response of CIDER with variability superimposed; the variability is taken from a random segment of pre-industrial climate simulation. These runs with variability can even form their own ensemble, for direct comparison with simulation ensembles of the same ensemble size. In principle, our method of adding variability is just one approach. CIDER could in the future be coupled with an emulator of internal variability (e.g., Link et al., 2019; Nath et al., 2022; Bassetti et al., 2024) to generate the combination of forced and unforced response while keeping file size low.

While useful in its current form, CIDER still has room for development. At its current stage, CIDER outputs AOD, temperature, precipitation, and evaporation fields. Future iterations can include more variables of interest that linearly scale reasonably well with the above (e.g., deposition of SO_2, heat extremes, precipitation extremes). Also, even though CIDER currently provides monthly-resolved climate output, it lacks a seasonal cycle. In theory, CIDER's climate module could be expanded to include unique dynamics for each month or season. Additionally, as Fig. 3 shows, the current form of CIDER does not capture AMOC dynamics. An additional set of dynamics could be integrated into CIDER to better estimate the ocean response to different strategies of SAI.

For fitting its parameters, CIDER currently uses optimization to reduce RMSE relative to its training data set, but future steps may include taking a Bayesian approach to parameter tuning (e.g., Dorheim et al., 2020). However, the natural variability present in the training data is not the only source of uncertainty. CIDER has several sources of uncertainty, namely in the parameters it fits, its parametric form, and the model it fits. CIDER's simplified form (described in Section 2a) does not account for all dynamics in CESM2 and UKESM1, and thus differences will appear even in the best-fit parameters. There is potential for the model parametric form to both not account for all the dynamics involved and not account for all sources of nonlinearity. Both of these lead to some residual differences relative to the training and testing data even with the best fit parameters. Furthermore, changing the relative weighting on the different simulations in the training data set will result in different best-fit parameters. The emulator in Farley et al. (2024) uses a modified version of EVA-H (Aubry et al., 2020) as its aerosol module, and it is able to capture the AOD responses of 0.5, 1.0, and 1.5 above PI very well. Farley et al. (2024)'s emulator uses the same climate variable dynamics module as the one in this paper, and it has the same issue with nonlinearity to different amounts of forcing that one can see in Fig. 2 but especially Fig. 4. Substituting in other dynamic models for the aerosol, climate variable, pattern scaling, and pattern-combining modules could yield better results. Doing so could also allow one to glean more dynamical information from the same emulator run (e.g., stratospheric residence time of the aerosols as in Toohey et al., 2024) or capture AMOC dynamics. Lastly, CIDER trains to fit the training data, which comes from a particular climate model or models, in our case CESM2 and UKESM1. By definition, climate features which these models do not capture well, CIDER will not capture well either. Future steps to address this could include training and testing CIDER onto a wider ensemble of different models and for all of their emulated outputs to be available in response to the same input, integrating a robust representation of inter-model uncertainties that could be provided together with the mean response values.

As a final note, it is possible to substitute in a machine learning model for any of CIDER's dynamic modules, but some caution is warranted. For instance, if one only saw Fig. 4h or 4i, one could conclude that UKESM1's multi-objective simulations are well-estimated and then place too much confidence in this reduced order model. Machine learning's tendency to overfit data

https://doi.org/10.5194/egusphere-2025-1830
Preprint. Discussion started: 21 May 2025

while often not allowing to explain the results only makes this phenomenon worse. It is only because we can break CIDER into its component parts, run diagnostics, and explain each parameter within that we can draw accurate conclusions on CIDER's performance and find areas for improvement.

Building an emulator is an iterative process, and we expect future iterations to improve on the various aspects we mentioned above, as well as by potentially including other forms of Climate Intervention (i.e., MCB, space mirrors). CIDER and all the code to reproduce our results is made available at https://doi.org/10.5281/zenodo.15277177. A web-based version will be soon made available at https://simulator.reflective.org/ (Beal et al., 2025).

Code and data availability. Data and code that support the findings of this study can be found at https://doi.org/10.5281/zenodo.15277104.

https://doi.org/10.5194/egusphere-2025-1830
Preprint. Discussion started: 21 May 2025

Appendix A

A1

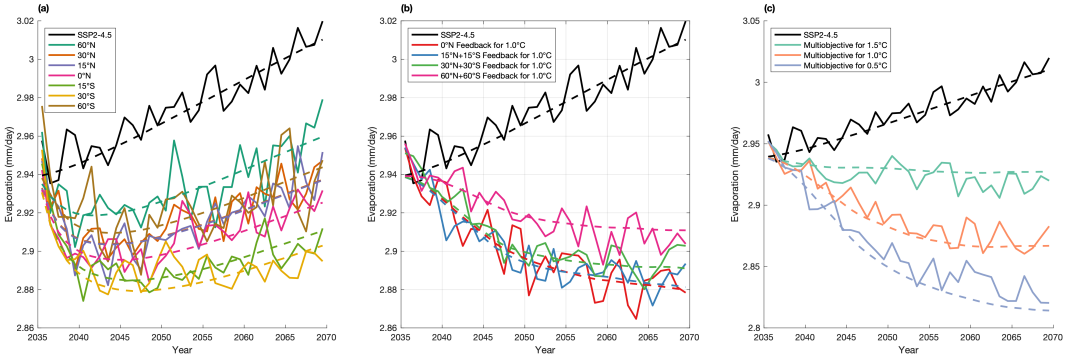

Figure A1. CESM2 (solid line) global mean responses of evaporation along with CIDER emulations of the same (dashed line). (a) shows the responses of the fixed injection (training data), (b) shows the responses of the symmetric injection runs for 1.0°C above PI (also training data), and (c) shows the responses of the multi-objective runs (validation data).

A2

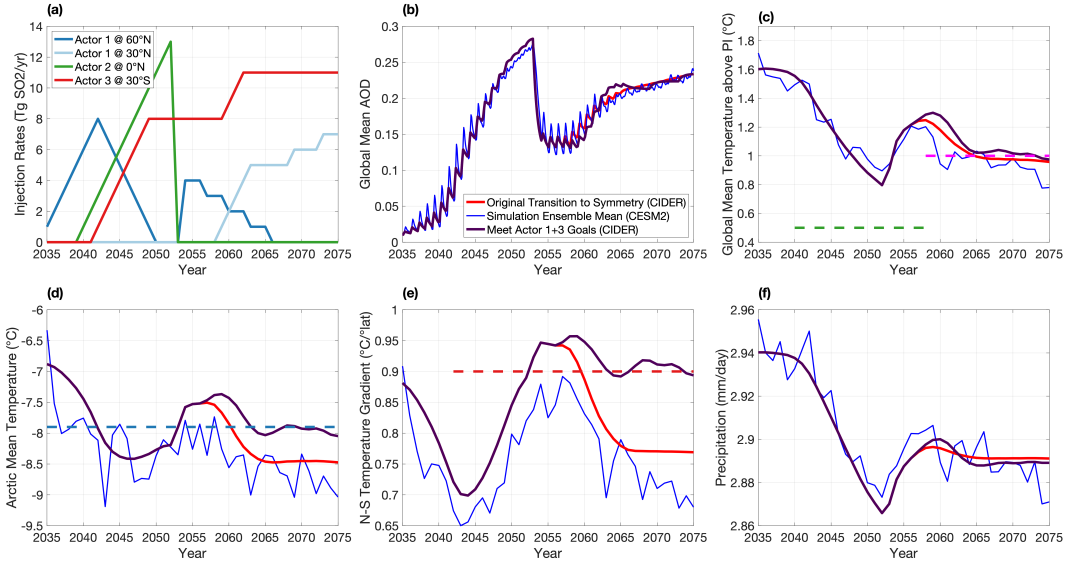

Figure A2. Example multi-actor uncoordinated scenario in CESM2 and emulated with CIDER from Section 2.3, along with a non-symmetric strategy that fulfills the individual goals of Actor 1 and 3.

https://doi.org/10.5194/egusphere-2025-1830
Preprint. Discussion started: 21 May 2025

Author contributions. JF prepared the manuscript with assistance from all co-authors. JF designed CIDER with supervision and assistance from DGM and DV. JF, DGM, DV, BK, and EB ran and assisted in assisted in acquiring various portions of the CESM2-WACCM6 output for training and validation. DV, AD, and MH ran and assisted in assisted in acquiring various portions of the UKESM1.0 output for training and validation.

Competing interests. The authors declare that they have no conflict of interest.

Acknowledgements. The CESM project is supported primarily by the National Science Foundation. High-performance computing was provided by NSF NCAR's Computational and Information Systems Laboratory (https://doi.org/10.5065/D6RX99HX), sponsored by the National Science Foundation. This work was partially supported by a grant from the Quadrature Climate Foundation. Support for JF was also provided by the Cornell Atkinson Center for Sustainability. Support for BK was provided in part by NOAA's Climate Program Office, Earth's Radiation Budget (ERB) (Grant NA22OAR4310479), and the Indiana University Environmental Resilience Institute. The Pacific Northwest National Laboratory is operated for the US Department of Energy by Battelle Memorial Institute under contract DE-AC05-76RL01830. Support for EMB has been provided by the National Oceanic and Atmospheric Administration (NOAA) cooperative agreement NA22OAR4320151 and the NOAA Earth Radiative Budget (ERB) program. AD's contribution was funded by the Natural Environment Research Council (NERC) London Doctoral Training Partnership (DTP) Grant NE/S007229/1. MH is funded by SilverLining through the Safe Climate Research Initiative.

https://doi.org/10.5194/egusphere-2025-1830
Preprint. Discussion started: 21 May 2025

References

Aubry, T. J., Toohey, M., Marshall, L., Schmidt, A., and Jellinek, A. M.: A New Volcanic Stratospheric Sulfate Aerosol Forcing Emulator (EVA_H): Comparison With Interactive Stratospheric Aerosol Models, Journal of Geophysical Research: Atmospheres, 125, e2019JD031 303, https://doi.org/10.1029/2019JD031303, 2020.

Bassetti, S., Hutchinson, B., Tebaldi, C., and Kravitz, B.: DiffESM: Conditional Emulation of Temperature and Precipitation in Earth System Models With 3D Diffusion Models, Journal of Advances in Modeling Earth Systems, 16, e2023MS004 194, https://doi.org/10.1029/2023MS004194, 2024.

Beall, C. M., Irvin, J. A., Dexheimer, J., Gruener, D., Ng, A. Y., MacMartin, D. G., and Visioni, D.: 1 The Stratospheric Aerosol Injection (SAI) Simulator: An Open- 2 Source Web Tool for Exploring Climate and SAI Deployment 3 Scenarios.

Bednarz, E. M., Visioni, D., Richter, J. H., Butler, A. H., and MacMartin, D. G.: Impact of the Latitude of Stratospheric Aerosol Injection on the Southern Annular Mode, Geophysical Research Letters, 49, e2022GL100 353, https://doi.org/10.1029/2022GL100353, 2022.

Bednarz, E. M., Visioni, D., Butler, A. H., Kravitz, B., MacMartin, D. G., and Tilmes, S.: Potential Non-Linearities in the High Latitude Circulation and Ozone Response to Stratospheric Aerosol Injection, Geophysical Research Letters, 50, e2023GL104 726, https://doi.org/10.1029/2023GL104726, 2023a.

Bednarz, E. M., Visioni, D., Kravitz, B., Jones, A., Haywood, J. M., Richter, J., MacMartin, D. G., and Braesicke, P.: Climate response to off-equatorial stratospheric sulfur injections in three Earth system models – Part 2: Stratospheric and free-tropospheric response, Atmospheric Chemistry and Physics, 23, 687–709, https://doi.org/10.5194/acp-23-687-2023, 2023b.

Bednarz, E. M., Goddard, P. B., MacMartin, D. G., Visioni, D., Bailey, D. A., and Danabasoglu, G.: Stratospheric Aerosol Injection could prevent future Atlantic Meridional Overturning Circulation decline, but injection location is key, https://doi.org/10.22541/essoar.173482135.52320055/v1, 2024.

Bell, C. M. and Keys, P. W.: Strategic logic of unilateral climate intervention, Environmental Research Letters, 18, 104 045, https://doi.org/10.1088/1748-9326/acf94b, 2023.

Brody, E., Visioni, D., Bednarz, E. M., Kravitz, B., MacMartin, D. G., Richter, J. H., and Tye, M. R.: Kicking the can down the road: understanding the effects of delaying the deployment of stratospheric aerosol injection, Environmental Research: Climate, 3, 035 011, https://doi.org/10.1088/2752-5295/ad53f3, 2024.

Dai, Z., Weisenstein, D. K., and Keith, D. W.: Tailoring Meridional and Seasonal Radiative Forcing by Sulfate Aerosol Solar Geoengineering, Geophysical Research Letters, 45, 1030–1039, https://doi.org/10.1002/2017GL076472, 2018.

Davis, N. A., Visioni, D., Garcia, R. R., Kinnison, D. E., Marsh, D. R., Mills, M., Richter, J. H., Tilmes, S., Bardeen, C. G., Gettelman, A., Glanville, A. A., MacMartin, D. G., Smith, A. K., and Vitt, F.: Climate, Variability, and Climate Sensitivity of "Middle Atmosphere" Chemistry Configurations of the Community Earth System Model Version 2, Whole Atmosphere Community Climate Model Version 6 (CESM2(WACCM6)), Journal of Advances in Modeling Earth Systems, 15, e2022MS003 579, https://doi.org/10.1029/2022MS003579, 2023.

Diao, C., Keys, P., Bell, C. M., Barnes, E. A., and Hurrell, J. W.: A model study exploring the decision loop between unilateral stratospheric aerosol injection scenario design and Earth system simulations, https://doi.org/10.22541/essoar.172901451.16665121/v1, 2024.

Dorheim, K., Link, R., Hartin, C., Kravitz, B., and Snyder, A.: Calibrating Simple Climate Models to Individual Earth System Models: Lessons Learned From Calibrating Hector, Earth and Space Science, 7, e2019EA000 980, https://doi.org/10.1029/2019EA000980, 2020.

https://doi.org/10.5194/egusphere-2025-1830
Preprint. Discussion started: 21 May 2025

Farley, J., MacMartin, D. G., Visioni, D., and Kravitz, B.: Emulating inconsistencies in stratospheric aerosol injection, Environmental Research: Climate, 3, 035 012, https://doi.org/10.1088/2752-5295/ad519c, 2024.

Henry, M., Haywood, J., Jones, A., Dalvi, M., Wells, A., Visioni, D., Bednarz, E. M., MacMartin, D. G., Lee, W., and Tye, M. R.: Comparison of UKESM1 and CESM2 simulations using the same multi-target stratospheric aerosol injection strategy, Atmospheric Chemistry and Physics, 23, 13 369–13 385, https://doi.org/10.5194/acp-23-13369-2023, 2023.

Henry, M., Bednarz, E. M., and Haywood, J.: How does the latitude of stratospheric aerosol injection affect the climate in UKESM1?, Atmospheric Chemistry and Physics, 24, 13 253–13 268, https://doi.org/10.5194/acp-24-13253-2024, 2024.

Heyen, D., Horton, J., and Moreno-Cruz, J.: Strategic implications of counter-geoengineering: Clash or cooperation?, Journal of Environmental Economics and Management, 95, 153–177, https://doi.org/10.1016/j.jeem.2019.03.005, 2019.

Hueholt, D. M., Barnes, E. A., Hurrell, J. W., and Morrison, A. L.: Speed of environmental change frames relative ecological risk in climate change and climate intervention scenarios, Nature Communications, 15, 3332, https://doi.org/10.1038/s41467-024-47656-z, 2024.

Jones, A., Haywood, J. M., Alterskjær, K., Boucher, O., Cole, J. N. S., Curry, C. L., Irvine, P. J., Ji, D., Kravitz, B., Egill Kristjánsson, J., Moore, J. C., Niemeier, U., Robock, A., Schmidt, H., Singh, B., Tilmes, S., Watanabe, S., and Yoon, J.: The impact of abrupt suspension of solar radiation management (termination effect) in experiment G2 of the Geoengineering Model Intercomparison Project (GeoMIP), Journal of Geophysical Research: Atmospheres, 118, 9743–9752, https://doi.org/10.1002/jgrd.50762, 2013.

Keith, D. W. and MacMartin, D. G.: A temporary, moderate and responsive scenario for solar geoengineering, Nature Climate Change, 5, 201–206, https://doi.org/10.1038/nclimate2493, 2015.

Keys, P. and Bell, C.: Designing a scenario of unilateral climate intervention, https://doi.org/10.31223/X56T3P, 2024.

Keys, P. W., Barnes, E. A., Diffenbaugh, N. S., Hurrell, J. W., and Bell, C. M.: Potential for perceived failure of stratospheric aerosol injection deployment, Proceedings of the National Academy of Sciences, 119, e2210036 119, https://doi.org/10.1073/pnas.2210036119, 2022.

Kravitz, B., MacMartin, D. G., Wang, H., and Rasch, P. J.: Geoengineering as a design problem, Earth System Dynamics, 7, 469–497, https://doi.org/10.5194/esd-7-469-2016, 2016.

Laakso, A., Kokkola, H., Partanen, A.-I., Niemeier, U., Timmreck, C., Lehtinen, K. E. J., Hakkarainen, H., and Korhonen, H.: Radiative and climate impacts of a large volcanic eruption during stratospheric sulfur geoengineering, Atmospheric Chemistry and Physics, 16, 305–323, https://doi.org/10.5194/acp-16-305-2016, 2016.

Latham, J., Rasch, P. J., and Launder, B.: Climate engineering: exploring nuances and consequences of deliberately altering the Earth's energy budget, Philosophical Transactions of the Royal Society A: Mathematical, Physical and Engineering Sciences, 372, 20140 050, https://doi.org/10.1098/rsta.2014.0050, 2014.

Lee, W. R., MacMartin, D. G., Visioni, D., Kravitz, B., Chen, Y., Moore, J. C., Leguy, G., Lawrence, D. M., and Bailey, D. A.: High-Latitude Stratospheric Aerosol Injection to Preserve the Arctic, Earth's Future, 11, e2022EF003 052, https://doi.org/10.1029/2022EF003052, 2023.

Link, R., Snyder, A., Lynch, C., Hartin, C., Kravitz, B., and Bond-Lamberty, B.: Fldgen v1.0: an emulator with internal variability and space–time correlation for Earth system models, Geoscientific Model Development, 12, 1477–1489, https://doi.org/10.5194/gmd-12-1477-2019, 2019.

MacMartin, D. G. and Kravitz, B.: Dynamic climate emulators for solar geoengineering, Atmospheric Chemistry and Physics, 16, 15 789–15 799, https://doi.org/10.5194/acp-16-15789-2016, 2016.

MacMartin, D. G., Kravitz, B., Keith, D. W., and Jarvis, A.: Dynamics of the coupled human–climate system resulting from closed-loop control of solar geoengineering, Climate Dynamics, 43, 243–258, https://doi.org/10.1007/s00382-013-1822-9, 2014.

https://doi.org/10.5194/egusphere-2025-1830
Preprint. Discussion started: 21 May 2025

MacMartin, D. G., Visioni, D., Kravitz, B., Richter, J., Felgenhauer, T., Lee, W. R., Morrow, D. R., Parson, E. A., and Sugiyama, M.: Scenarios for modeling solar radiation modification, Proceedings of the National Academy of Sciences, 119, e2202230 119, https://doi.org/10.1073/pnas.2202230119, 2022.

McLaren, D.: "It's Not the Climate, Stupid": Exploring Nonideal Scenarios for Solar Geoengineering Development, Ethics & International Affairs, 38, 255–274, https://doi.org/10.1017/S089267942400025X, 2024.

Meier, F. and Traeger, C.: Solar Geoengineering in a Regional Analytic Climate Economy.

Meinshausen, M., Nicholls, Z. R. J., Lewis, J., Gidden, M. J., Vogel, E., Freund, M., Beyerle, U., Gessner, C., Nauels, A., Bauer, N., Canadell, J. G., Daniel, J. S., John, A., Krummel, P. B., Luderer, G., Meinshausen, N., Montzka, S. A., Rayner, P. J., Reimann, S., Smith, S. J., Van Den Berg, M., Velders, G. J. M., Vollmer, M. K., and Wang, R. H. J.: The shared socio-economic pathway (SSP) greenhouse gas concentrations and their extensions to 2500, Geoscientific Model Development, 13, 3571–3605, https://doi.org/10.5194/gmd-13-3571-2020, 2020.

Morrissey, W.: Avoiding atmospheric anarchy: Geoengineering as a source of interstate tension, Environment and Security, 2, 291–315, https://doi.org/10.1177/27538796231221597, 2024.

Nath, S., Lejeune, Q., Beusch, L., Seneviratne, S. I., and Schleussner, C.-F.: MESMER-M: an Earth system model emulator for spatially resolved monthly temperature, Earth System Dynamics, 13, 851–877, https://doi.org/10.5194/esd-13-851-2022, 2022.

Pereira, L. M., Morrow, D. R., Aquila, V., Beckage, B., Beckbesinger, S., Beukes, L., Buck, H. J., Carlson, C. J., Geden, O., Jones, A. P., Keller, D. P., Mach, K. J., Mashigo, M., Moreno-Cruz, J. B., Visioni, D., Nicholson, S., and Trisos, C. H.: From fAIrplay to climate wars: making climate change scenarios more dynamic, creative, and integrative, Ecology and Society, 26, art30, https://doi.org/10.5751/ES-12856-260430, 2021.

Quaglia, I., Visioni, D., Bednarz, E. M., MacMartin, D. G., and Kravitz, B.: The Potential of Stratospheric Aerosol Injection to Reduce the Climatic Risks of Explosive Volcanic Eruptions, Geophysical Research Letters, 51, e2023GL107 702, https://doi.org/10.1029/2023GL107702, 2024.

Richter, J. H., Visioni, D., MacMartin, D. G., Bailey, D. A., Rosenbloom, N., Dobbins, B., Lee, W. R., Tye, M., and Lamarque, J.-F.: Assessing Responses and Impacts of Solar climate intervention on the Earth system with stratospheric aerosol injection (ARISE-SAI): protocol and initial results from the first simulations, Geoscientific Model Development, 15, 8221–8243, https://doi.org/10.5194/gmd-15-8221-2022, 2022.

Rooney-Varga, J. N., Kapmeier, F., Sterman, J. D., Jones, A. P., Putko, M., and Rath, K.: The Climate Action Simulation, Simulation & Gaming, 51, 114–140, https://doi.org/10.1177/1046878119890643, 2020.

Smith, C. J., Forster, P. M., Allen, M., Leach, N., Millar, R. J., Passerello, G. A., and Regayre, L. A.: FAIR v1.3: a simple emissions-based impulse response and carbon cycle model, Geoscientific Model Development, 11, 2273–2297, https://doi.org/10.5194/gmd-11-2273-2018, 2018.

Smith, W., Bhattarai, U., MacMartin, D. G., Lee, W. R., Visioni, D., Kravitz, B., and Rice, C. V.: A subpolar-focused stratospheric aerosol injection deployment scenario, Environmental Research Communications, 4, 095 009, https://doi.org/10.1088/2515-7620/ac8cd3, 2022.

Sovacool, B. K., Baum, C., and Low, S.: The next climate war? Statecraft, security, and weaponization in the geopolitics of a low-carbon future, Energy Strategy Reviews, 45, 101 031, https://doi.org/10.1016/j.esr.2022.101031, 2023.

Tebaldi, C., Snyder, A., and Dorheim, K.: STITCHES: creating new scenarios of climate model output by stitching together pieces of existing simulations, Earth System Dynamics, 13, 1557–1609, https://doi.org/10.5194/esd-13-1557-2022, 2022.

https://doi.org/10.5194/egusphere-2025-1830
Preprint. Discussion started: 21 May 2025

Tilmes, S., Richter, J. H., Mills, M. J., Kravitz, B., MacMartin, D. G., Vitt, F., Tribbia, J. J., and Lamarque, J.: Sensitivity of Aerosol Distribution and Climate Response to Stratospheric SO_2 Injection Locations, Journal of Geophysical Research: Atmospheres, 122, https://doi.org/10.1002/2017JD026888, 2017.

Tilmes, S., Richter, J. H., Kravitz, B., MacMartin, D. G., Mills, M. J., Simpson, I. R., Glanville, A. S., Fasullo, J. T., Phillips, A. S., Lamarque, J.-F., Tribbia, J., Edwards, J., Mickelson, S., and Ghosh, S.: CESM1(WACCM) Stratospheric Aerosol Geoengineering Large Ensemble Project, Bulletin of the American Meteorological Society, 99, 2361–2371, https://doi.org/10.1175/BAMS-D-17-0267.1, 2018.

Tilmes, S., MacMartin, D. G., Lenaerts, J. T. M., Van Kampenhout, L., Muntjewerf, L., Xia, L., Harrison, C. S., Krumhardt, K. M., Mills, M. J., Kravitz, B., and Robock, A.: Reaching 1.5 and 2.0 °C global surface temperature targets using stratospheric aerosol geoengineering, Earth System Dynamics, 11, 579–601, https://doi.org/10.5194/esd-11-579-2020, 2020.

Toohey, M., Jia, Y., Khanal, S., and Tegtmeier, S.: Stratospheric residence time and the lifetime of volcanic stratospheric aerosols, Atmos. Chem. Phys., 2025.

Trisos, C. H., Amatulli, G., Gurevitch, J., Robock, A., Xia, L., and Zambri, B.: Potentially dangerous consequences for biodiversity of solar geoengineering implementation and termination, Nature Ecology & Evolution, 2, 475–482, https://doi.org/10.1038/s41559-017-0431-0, 2018.

Visioni, D., Bednarz, E. M., Lee, W. R., Kravitz, B., Jones, A., Haywood, J. M., and MacMartin, D. G.: Climate response to off-equatorial stratospheric sulfur injections in three Earth system models – Part 1: Experimental protocols and surface changes, Atmospheric Chemistry and Physics, 23, 663–685, https://doi.org/10.5194/acp-23-663-2023, 2023a.

Visioni, D., Bednarz, E. M., MacMartin, D. G., Kravitz, B., and Goddard, P. B.: The Choice of Baseline Period Influences the Assessments of the Outcomes of Stratospheric Aerosol Injection, Earth's Future, 11, e2023EF003 851, https://doi.org/10.1029/2023EF003851, 2023b.

Weitzman, M. L.: A Voting Architecture for the Governance of Free-Driver Externalities, with Application to Geoengineering, The Scandinavian Journal of Economics, 117, 1049–1068, https://doi.org/10.1111/sjoe.12120, 2015.

Wheeler, L., Wagman, B., Smith, W., Davies, P., Cook, B., Brunell, S., Glen, A., Hackenburg, D., Lien, J., Shand, L., and Zeitler, T.: Design and simulation of a logistically constrained high-latitude, low-altitude stratospheric aerosol injection scenario in the Energy Exascale Earth System Model (E3SM), Environmental Research Letters, 20, 044 011, https://doi.org/10.1088/1748-9326/adba01, 2025.

Zhang, Y., MacMartin, D. G., Visioni, D., and Kravitz, B.: How large is the design space for stratospheric aerosol geoengineering?, Earth System Dynamics, 13, 201–217, https://doi.org/10.5194/esd-13-201-2022, 2022.

Zhang, Y., MacMartin, D. G., Visioni, D., Bednarz, E. M., and Kravitz, B.: Hemispherically symmetric strategies for stratospheric aerosol injection, Earth System Dynamics, 15, 191–213, https://doi.org/10.5194/esd-15-191-2024, 2024.